RAPPORT FINAL
2006


Sous-projet SC13


# Red-bed copper deposits of the Quebec Appalachians


Par


## Alexandre Raphael Cabral et Georges Beaudoin

Département de Géologie et génie géologique, Université Laval, Québec, G1K 7P4

Soumis à l'administration de DIVEX
mars 2006 - Montréal

**Abstract**

This report presents the final results of the project 'red-bed copper deposits of the Quebec Appalachians'. Emphasis has been placed on two deposits: 1) the Transfiguration Cu–Pb–Zn–Ag deposit, associated with continental red beds of the Lower Silurian Robitaille Formation; 2) the Mont Alexandre native copper, hosted in basaltic flows of the Upper Silurian Lac McKay Member. Geochemical, petrographical and geological data suggest two mineralisation stages for Transfiguration: i) ponding of relatively reduced groundwater over the Taconian unconformity, recorded by a nodular calcrete horizon, and early pyrite via bacterial sulphate reduction; ii) pseudomorphic replacement of early pyrite by chalcopyrite, as well as sulphide via thermochemical sulphate reduction, in grey (reduced) sandstone as a result of fault-controlled percolation and interaction of a cupriferous fluid *per descensum* from the red-bed sequence and a hydrocarbon-bearing fluid *per ascensum* from the Cambro-Ordovician basement. Faulting and concurrent fluid migration are tentatively ascribed to the Salinic extensional tectonics.
The volcanic-hosted copper deposits of the Mont Alexandre region, exemplified by the "Triangle d'Argent" quarry, are not 'volcanic red-bed' *sensu stricto* since the volcanic flows were not oxidised in subaerial environment. Instead, the basaltic rocks were spilitised. Heated sea water induced hydrothermal alteration (albitization, chloritization and hematitization) and leached metals from magmatic silicates, particularly from native copper-bearing plagioclase, to form the Cu–Ag epigenetic mineralisation.

## INTRODUCTION

Sediment-hosted stratiform cupriferous deposits account for approximately 23% of the world's copper production and known reserves, and are important sources of silver and cobalt. Some deposits also contain by-product gold, uranium and platinum-group elements (Kirkham 1989, Brown 1992, Hitzman *et al.* 2005). Economically significant cupriferous deposits in the Gaspé Peninsula, Quebec Appalachians, are hitherto associated with porphyritic intrusions and skarns, particularly in the Murdochville area (*e.g.*, Bellehumeur & Valiquette 1993). There are, however, several occurrences of both sediment- and volcanic-hosted copper in Lac Témiscouata and Mont Alexandre areas, respectively, that remain poorly documented despite their potential for mineral diversification in the region.

The current project has focused on a better understanding of two relevant occurrences (Transfiguration and Mont Alexandre) of red-bed copper in the Gaspé Peninsula (Fig. 1). This report presents the results of geochemical and mineralogical investigations carried out since August 2004.

## TRANSFIGURATION

*Geological setting and deposit geology*

Initially identified as galena-cemented sandstone (Schrijver & Beaudoin 1987), mineralisation at Transfiguration (Fig. 1) was subsequently characterised as Cu–Pb–Zn–Ag deposit associated with continental red beds. The Transfiguration red-bed sequence are Lower Silurian rocks of the Robitaille Formation deposited on deformed pre-Taconic rocks of the Humber Zone, above the Taconian unconformity (Bourque *et al.* 1995, Malo 2004).

The Robitaille Formation is part of the lower terrigenous assemblage of the Chaleurs Group (Bourque *et al.* 1995, 2001). In the Lake Témiscouata region, the Robitaille Formation represents the terrestrial succession of a shallowing upward sedimentation following Taconian orogeny (Fig. 2). The shallowing phase is recognised by the upward change from deep-water turbidite to shallow-water sediments (Cabano Group), and then from subaerial lava flows and volcaniclastic gravels (Pointe-aux-Trembles) to terrestrial red beds (Robitaille). Overlying the Robitaille Formation, the Sayabec Formation is a platformal limestone unit with lateral facies variation from peritidal mud flat to deeper water, nodular lime mud belt (Lavoie *et al.* 1992). The late Llandoverian to late Wenlockian Sayabec platform is the middle carbonate assemblage of the Chaleurs Group and corresponds to the peak of the first shallowing phase after the Taconian orogeny. The sea-level stability of the Sayabec platform ended with the influx of deep-water, fine-grained siliciclastic sediments (the upper terrigenous assemblage of the Chaleurs Group, *i.e*, Saint-Léon Formation and equivalents) during a late Wenlockian transgression. Following this transgression, extensional tectonics related to the Late Silurian–Early Devonian Salinic disturbance resulted in synsedimentary faulting concomitant with eustatic sea-level fall and subaerial erosion of the highest parts (Bourque 2001, Malo 2001).

The simplified deposit stratigraphy comprises, from bottom to top (Fig. 3): (a) sheared slate (Cambro-Ordovician basement, *i.e*, Trinité Group and Québec Supergroup); (b) calcrete nodules in greenish sandstone; (c) polymictic conglomerate; (d) greyish sandstone; and (e) reddish sandstone. The contact between the reddish and the greyish sandstone units is interdigitated, where reddish areas (i) are either rimmed by a greenish alteration halo within greyish
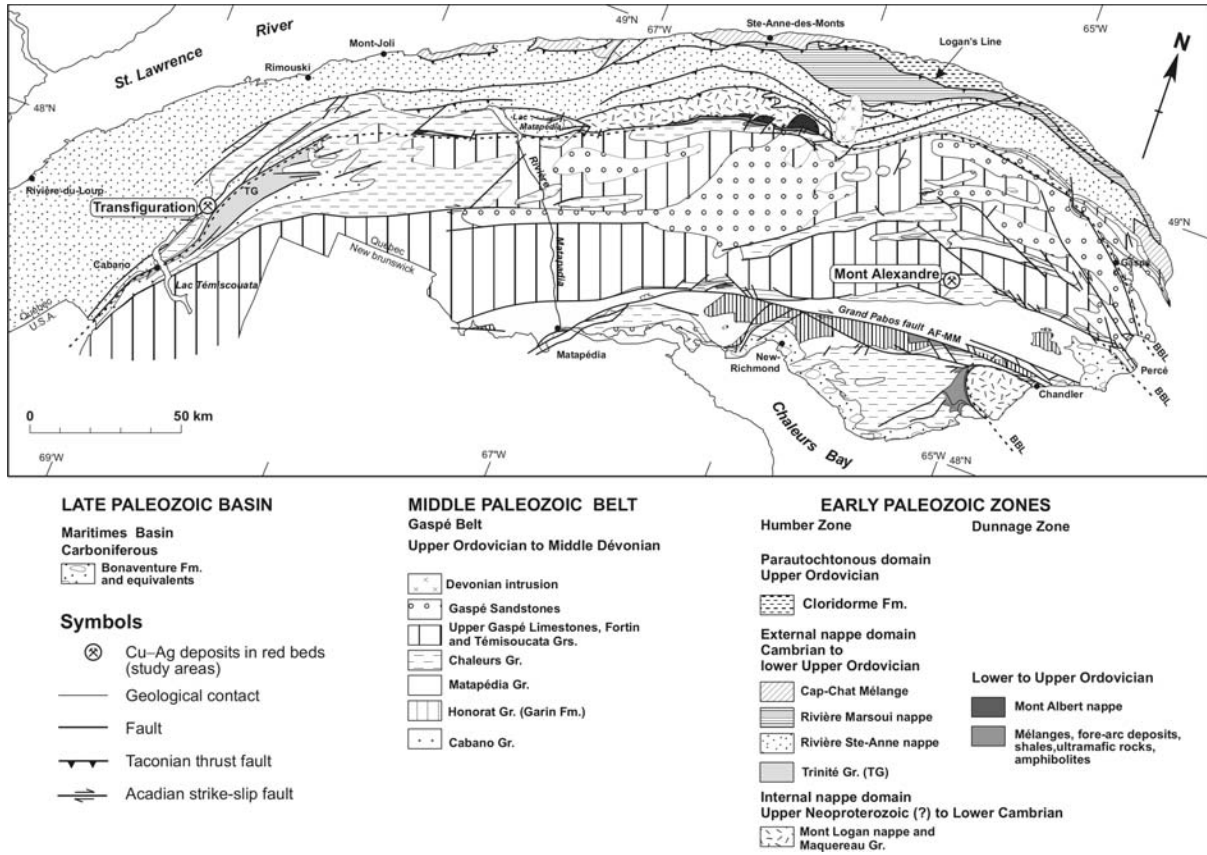
Fig. 1. Location of the cupriferous occurrences investigated (Transfiguration and Mont Alexandre) and major stratigraphic units of the Gaspé Appalachians (modified from Malo 2004).

sandstone (Fig. 4a), or (ii) envelop greyish portions upon which a reddish alteration halo is imprinted (Fig. 4b). The sandstones are quartz arenite, sub litharenite and quartzwacke and consist of fine-grained, moderately to poorly sorted detrital grains.

Intergranular illite and chlorite appear to characterise, respectively, the greyish and greenish sandstones. Both contain disseminated pyrite interstitial to detrital grains, in amounts varying from trace to a few modal per cent. In mineralised intervals, the greyish
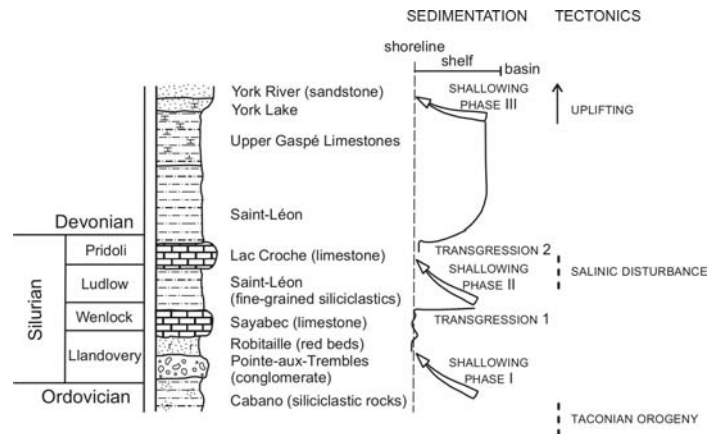


Fig. 2. Depositional environments during Silurian for the the Lake Témiscouata region (after Bourque *et al*. 1995).
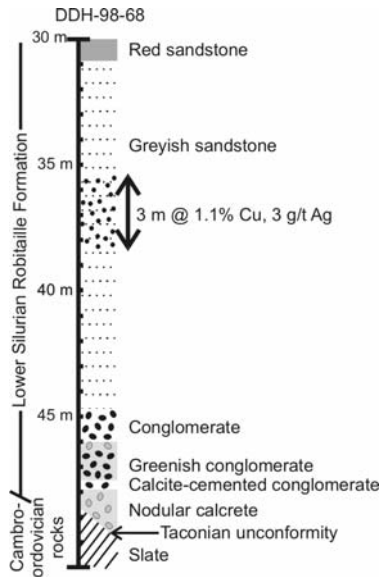
2

Fig. 3. Simplified deposit stratigraphy, Transfiguration.

sandstone exhibits displacive calcite growth (Fig. 5a), feldspar destruction and quartz dissolution by dolomite concurrent with chalcopyrite precipitation, with or without albite (Figs. 5b, c).

The calcrete nodules vary in width from a few millimetres to some centimetres and consist essentially of micritic and sparry calcite, with microstructures typical of alpha-type calcrete (Wright 1990). The microstructures include calcite-filled cracks (crystallaria) and floating grains (Fig. 6a), and circum-granular cracks (Fig. 6b). Barite in crystallaria (Fig. 6a), authigenic albite (Fig. 6c) and replacive pyrite (Fig. 6d), with or without minor galena and
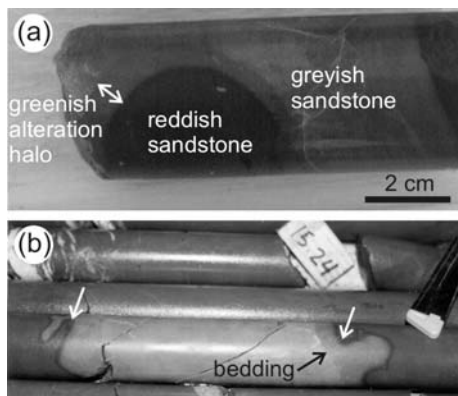


Fig. 4. (a) Greenish alteration halo on a nodule of reddish sandstone, which is bleached to greyish sandstone. Drill core 97-11, 8.70 m. (b) Reddish alteration obliterates greyish sandstone (arrows). Drill core 97-10, 18.2 m.
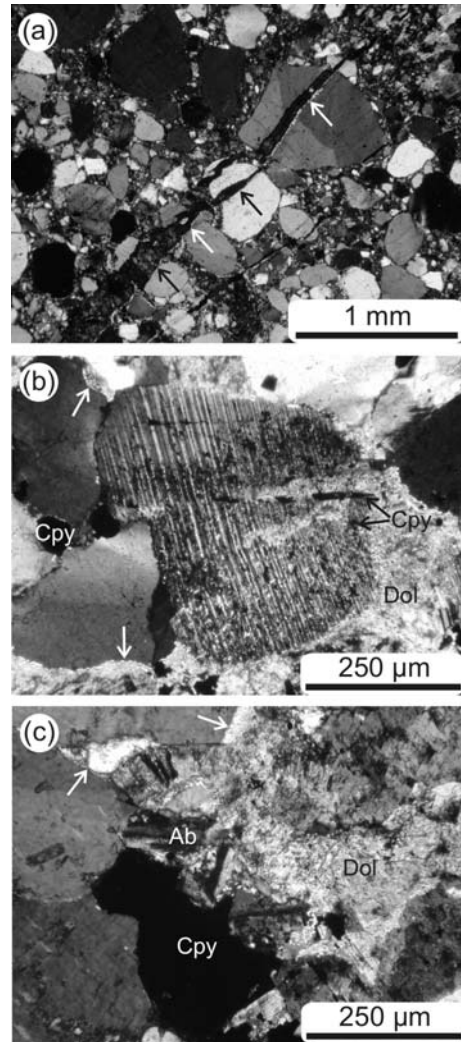


Fig. 5. Photomicrographs of greyish sandstone (plane-polarised light with crossed polars). (a) Feldspar destruction (centre) and chalcopyrite (Cpy) precipitation in dolomite cement between corroded detrital quartz (white arrows). (b) Displacive calcite in detrital quartz (arrows). (c) Etching of detrital quartz (arrows) with albite (Ab) and chalcopyrite (Cpy) deposition in dolomite cement.

sphalerite, are occasionally found in the calcrete nodules. Floating grains of detrital quartz are commonly etched (Fig. 6e) and, ultimately, replaced by coarse-grained calcite (Fig. 6f).

*Mineralisation*

Sulphide disseminations and minor veinlets make up the Transfiguration mineralisation, which is confined to the greyish sandstone and conglomerate between
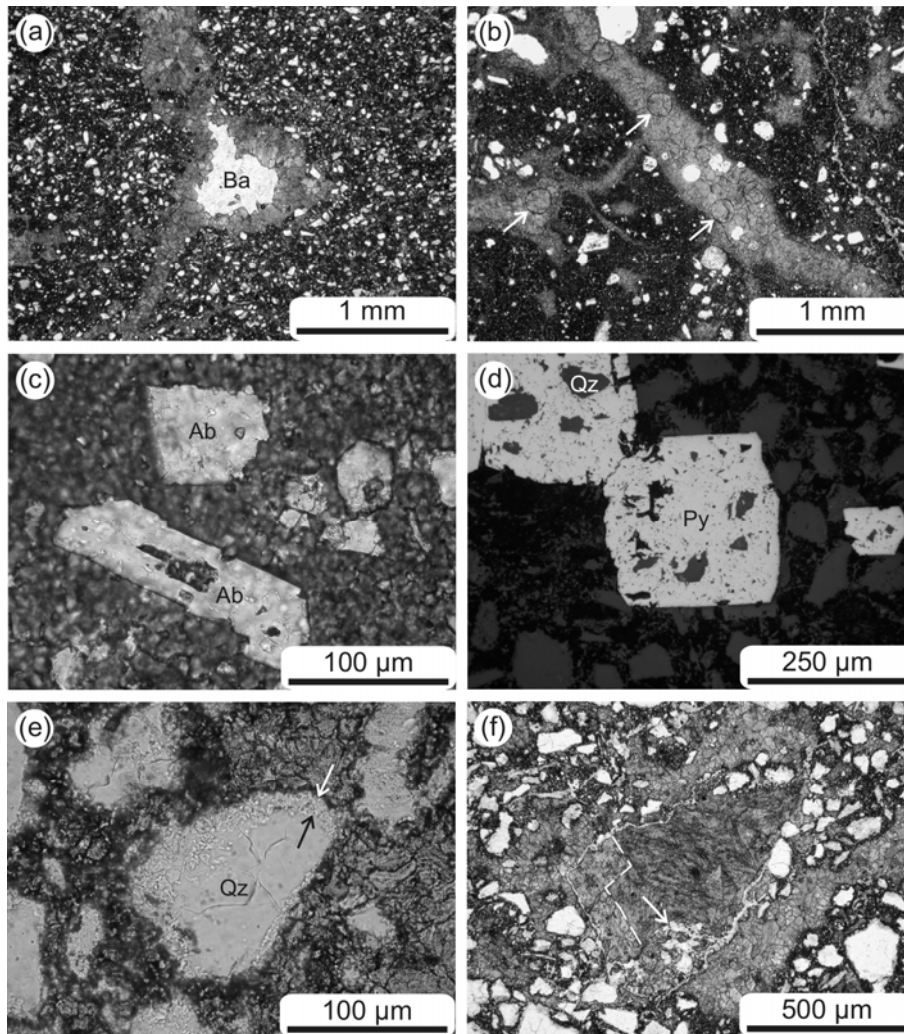
Fig 6. Photomicrographs of stained thin sections showing calcrete alpha fabrics (plane-polarised light, unless otherwise indicated). (a) Calcite-filled cracks (crystallaria) with barite (Ba, centre). (b) Crystallaria with circum-granular cracks (arrows) in micritic fabric of floating grains (white, mainly quartz). (c) Albite (Ab) in calcrete nodule. (d) Replacive pyrite (Py) with inclusions of corroded quartz (Qz) in floating fabric. Reflected light, air. (e) Etched margins (arrows) of detrital quartz in floating fabric. (f) Complete replacement of detrital quartz by coarse-grained calcite. Dashed line separates two calcite crystals and arrow points to relic quartz (white).

the Taconian unconformity and overlying red sandstone unit (Fig. 3). The contact between the calcrete horizon and the basement is sometimes marked (i) by breccias and calcite veins with which minor sulphide dissemination is associated, as well as (ii) by fault-related barite veins with sphalerite dissemination in the adjacent sandstone. There are mineralised intervals that tend to be enriched in lead and zinc [*e.g.*, 3.4 m @ 0.25% Cu, 3.0% Pb, 2.0% Zn, 18.2g/t Ag (Hupé 2001)]. The mineralisation is traced along 2 km and attains 13.9 m in width with 0.4% Cu and 5.3g/t Ag (Hupé 2001).

Disseminated sulphides are interstitial to detrital grains. Pyrite and, subordinately, marcasite are the earliest sulphides. Pyrite is replaced by chalcopyrite (Fig. 7a) and cross-cut by galena (Fig. 7b). This early pyrite is commonly plumbiferous, with Pb-rich core and Pb-poor margin discernible only under high-gain backscattered electron imaging (Fig. 7c). The lead content in pyrite is as high as 2.2 wt% and co-vary with iron (Fig. 7d). Galena also occurs as inclusions in authigenic albite (Fig. 7e). Chalcopyrite coexists with pyrite and albite in <2 mm-wide veins (Fig. 7f). Albite in veins hosts
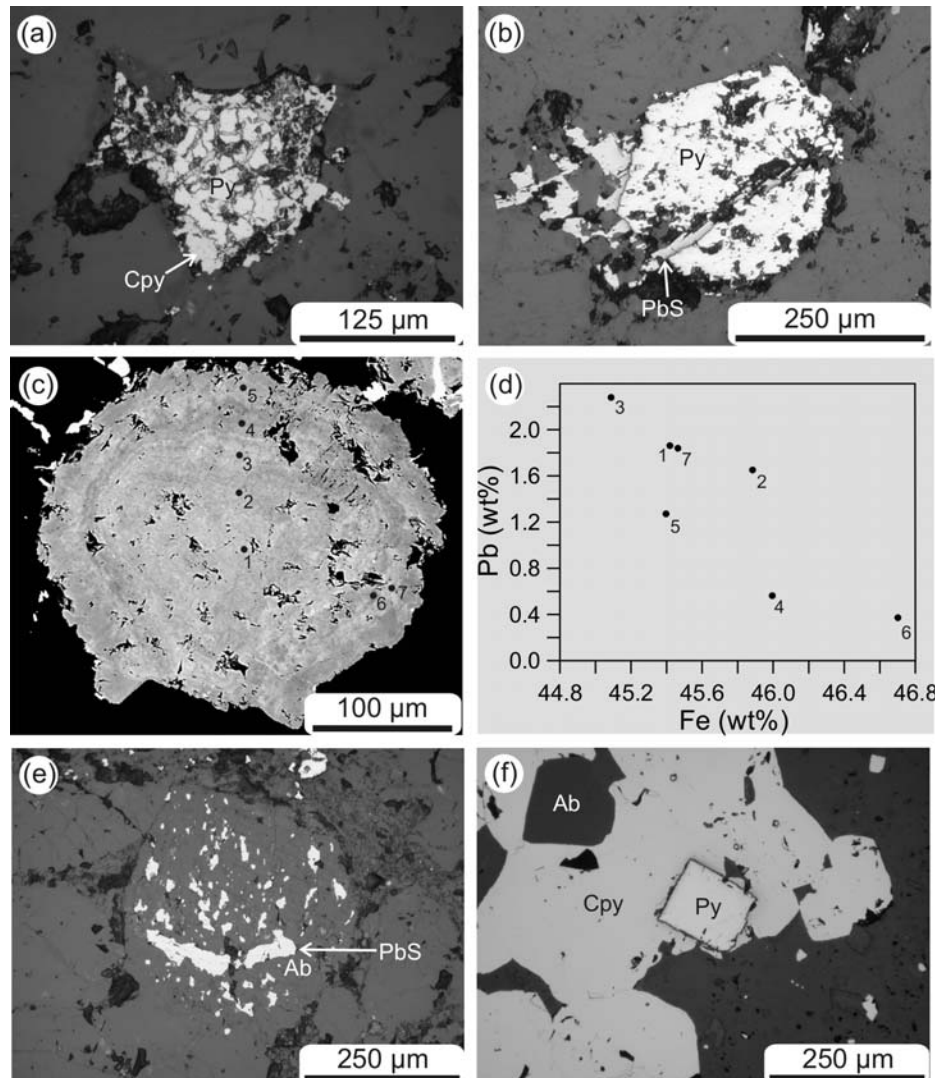
4

Fig. 7. Reflected-light microphotographs, air, unless otherwise stated. (a) Pyrite (Py) is pseudomorphically replaced by chalcopyrite (Cpy). (b) Pyrite (Py) is cross-cut by galena (PbS, light grey). (c) High-gain backscattered electron (BSE) image of plumbiferous pyrite showing Pb-poor (darker) and Pb-rich (lighter) growth bands. Numbers refer to electron-microprobe analyses in (d). (d) Fe vs. Pb plot of microanalyses indicated in (c). (e) Galena (PbS, white) in authigenic albite (Ab). (f) Veinlet chalcopyrite (Cpy) intergrown with pyrite (Py) and albite (Ab).

tiny (<5 μm), hydrocarbon-bearing fluid inclusions (Fig. 8).

Marcasite is locally the main iron sulphide. It occurs as isolated crystals and as aggregates, both partially inverted to pyrite. Pyrite after marcasite is porous and the pores appear to be filled by galena and a cupriferous phase, possibly chalcopyrite (Fig. 9). Marcasite hosts, and is cross-cut by, sphalerite containing up to 16 wt% Fe.

The major argentiferous phase is idaite, with up to 11 wt% Ag (Fig. 10). Idaite is found as tabular crystals and composite aggregates with chalcopyrite in the interstices of detrital grains. Other sulphides associated with chalcopyrite, probably as replacements, are compositionally analogous to $(Cu_{4.7},Fe_{1.3})_6 S_5$ and $(Cu_{5.7},Fe_{1.2})_7 S_5$. There is a Cu-rich, Ag-bearing phase similar in composition to geerite, located at the margin of idaite. The idaite of Figure 10 is surrounded by a narrow rim of argentiferous geerite-like phase. Pyrite and marcasite contain a few hundred ppm Ag (Fig. 9).
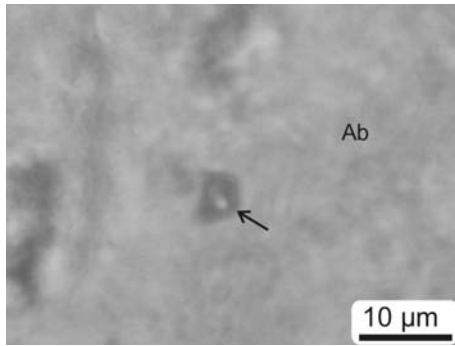
5

Fig. 8. Hydrocarbon-bearing fluid inclusion (dark, arrow) in authigenic albite (Ab) intergrown with veinlet chalcopyrite.

*Stable isotopes*

Bulk analyses of sulphide, sulphate and carbonate concentrates were performed at G.G. Hatch Isotope Laboratories, University of Ottawa. Sulphide $\delta^{34}S$ values display a wide range, from -19 to 25‰ with a mode at -15‰ (Fig. 11). The highest sulphide $\delta^{34}S$ value (25.1‰) is close to that of vein barite (26.2‰). Chalcopyrite intergrown with albite that hosts hydrocarbon-bearing fluid inclusions (Figs. 7f, 8) has low $\delta^{34}S$ values (-15.2 and -1.2‰).

Disseminated and vein carbonates and calcrete have $\delta^{13}C$ values ranging from -15.8 to -9.4‰, whereas $\delta^{18}O$ values range from 14.7 to 21.3‰ (Fig. 12).

**MONT ALEXANDRE**

*Geological setting and deposit geology*

Mont Alexandre is a major E–W-trending synclinal structure developed during the Acadian orogeny (Bourque & Lachambre 1980, Morin & Simard 1987). The core of the Mont Alexandre syncline consists predominantly of fine-grained siliciclastic rocks (mudstone and sandstone) of the Lower Devonian Indian Point Formation of the Chaleurs Group (Fig. 13). The underlying rocks are calcilutite and calcareous conglomerate of the West Point Formation. The volcanic pile is divided into two members: conglomerate and coarse-grained sandstone with minor basaltic rocks of the Mont Observation Member; and basaltic rocks with subordinate andesite, dacite and epiclastic rocks of the Upper Silurian Lac McKay Member (Bourque 1975). The basaltic rocks of the Lac McKay Member are interbedded with deep-water siliciclastic sediments (Bourque *et al*. 1995, Bourque 2001).
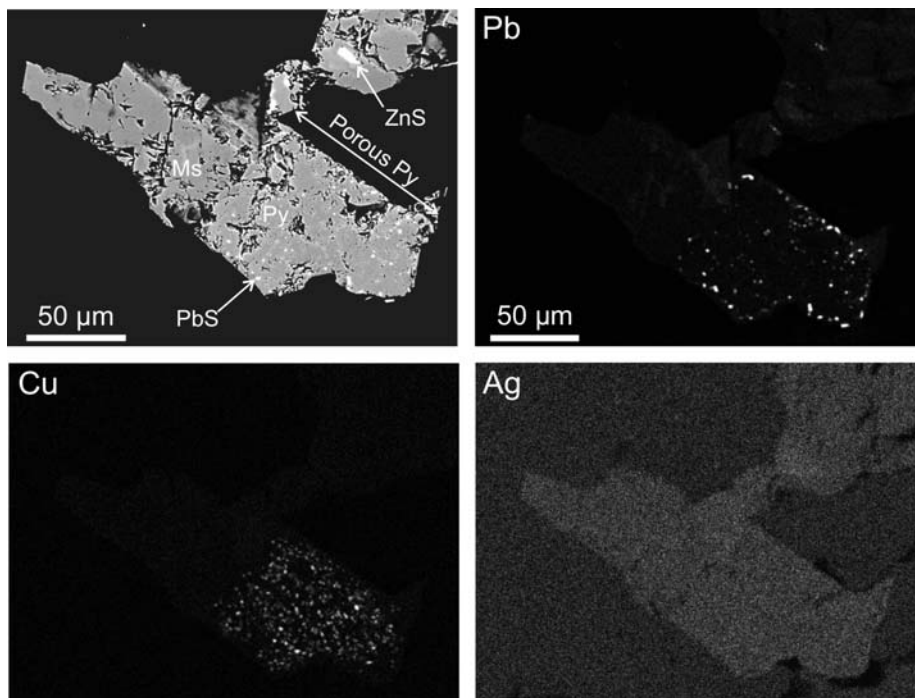


Fig. 9. BSE image of marcasite (Ms) inversion to porous pyrite (Py). X-ray mapping for Pb, Cu and Ag indicates that the pores are filled by galena and, possibly, chalcopyrite, and that silver is present in the range of a few hundred ppm.
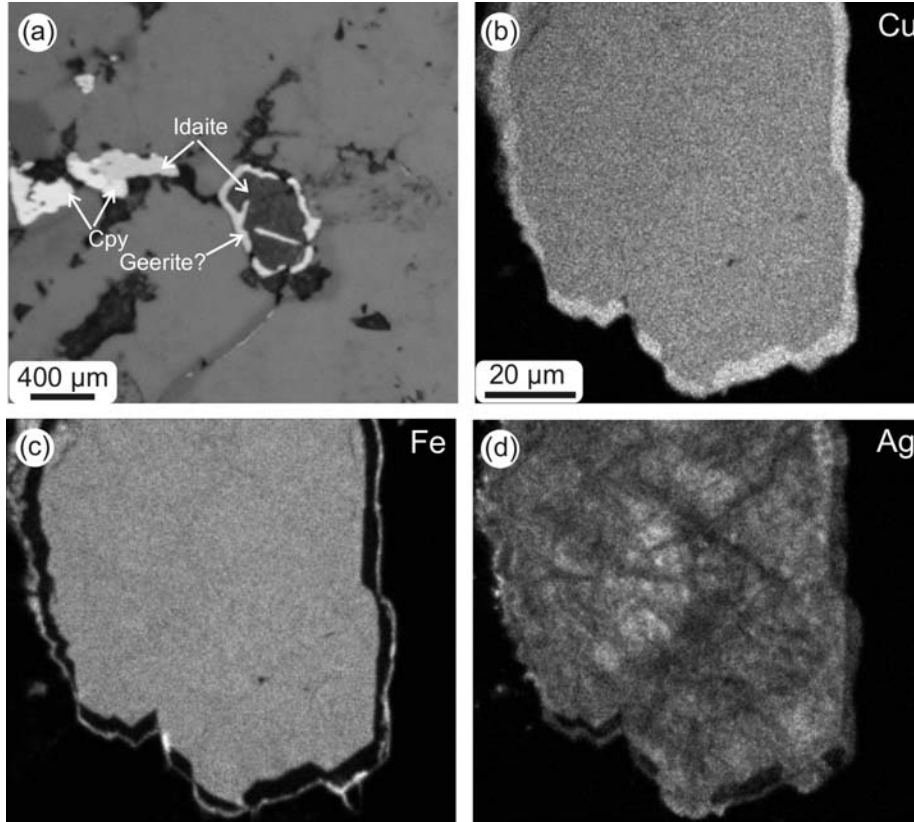
6

Fig. 10. (a) Reflected-light photomicrograph (air) of interstitial chalcopyrite  (Cpy) and idaite. X-ray mapping for Cu (b), Fe (c) and Ag (d) in idaite. *Vide* text for explanation.
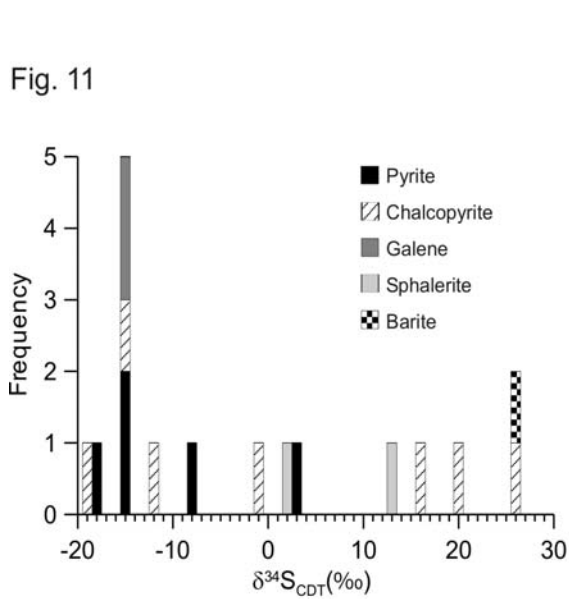


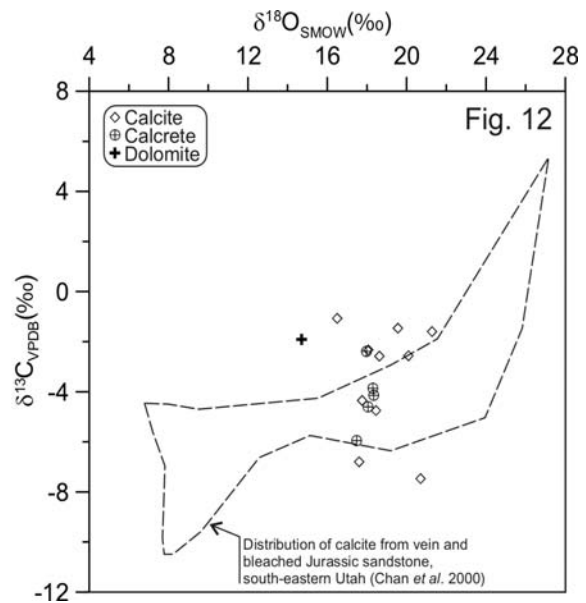Fig. 11. Histogram of $\delta^{34}$S values of sulphides and barite.



Fig. 12. $\delta^{13}$C vs. $\delta^{18}$O plot; *vide* discussion for explanation.
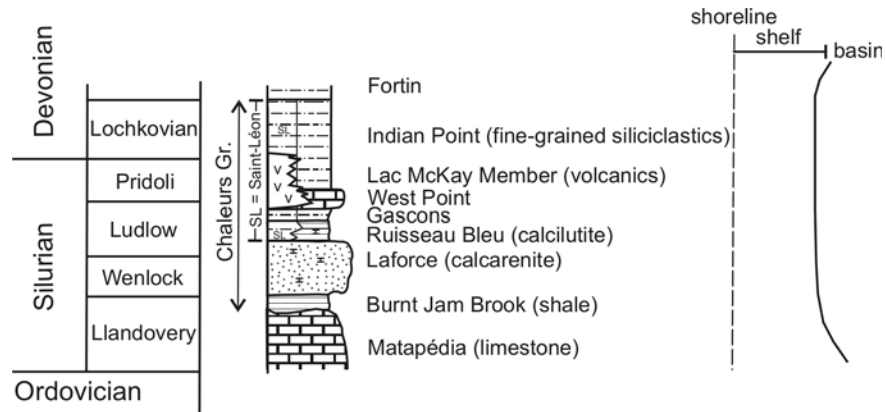
Fig. 13. Depositional environments during Silurian for the Mont Alexandre region (after Bourque & Lachambre 1980, Bourque 2001).

Prehnite–pumpellyite facies metamorphism affected the volcanic rocks (Bédard 1986a). Primary flow textures are preserved, but the rocks are pervasively altered to secondary minerals, such as albite, chlorite, epidote, calcite and quartz (Bédard 1986a, Dostal *et al*. 1993).

The Lac McKay lavas are mostly alkaline basalts (Laurent & Bélanger 1984, Bédard 1986b). The alkaline character is manifested by $Na_2O$ contents from 3.0 to 6.9 wt% and normative albite, although the abnormally high proportion of normative albite may be attributable to sodic alteration (Morin and Simard 1987). The lavas become more oxidised toward the top of the sequence (Bédard 1986b). The basalts were probably erupted during a tensional event in an orogenic foreland setting (Bédard 1986b, Dostal *et al*. 1993) and should represent an episode of intraplate volcanism during the Salinic disturbance (Malo 2001).

*Mineralisation*

Native copper mineralisation is known to be hosted in mafic volcanics of the Mont Alexandre area since 1936 (Jones 1938). Of the numerous occurrences of cupriferous mineralisation (Duffours 2000), that designated as "Triangle d'Argent" was worked for native copper. Its quarry exposes basaltic rocks overprinted by alteration, which is more intense in the central (mineralised) portion of the quarry (Fig. 14). The least altered basalt, immediately adjacent to the marginal zone of the quarry and furthest from the mineralised area (centre), is characterised by coarse-grained phenocrysts of turbid plagioclase in hematitic, cryptocrystalline groundmass. The porphyritic basalt is brecciated and cemented by ferruginous mass (Fig. 14a). This aphanitic material consists of fine-grained quartz, white mica, K-feldspar, hematite and zircon, and void-filling aggregates of chlorite and calcite, within a ferruginous groundmass.

Towards the centre of the quarry, plagioclase becomes albitized. Pseudomorphic chlorite after feldspar and other magmatic silicates are replaced by hematite (Figs. 15a, b). The chlorite has Fe/(Fe+Mg) ratios varying from 0.29 to 0.36, a range within that of the chlorite investigated by Cathelineau & Nieva (1985). Application of their chlorite geothermometer suggests temperatures between 155 to 182°C for chloritization at the Triangle d'Argent quarry. Radiating aggregates of fibrous albite fill in veinlets with yarrowite (Fig. 15c) and voids with chalcocite, malachite and barite (Fig. 15d). Calcite-filled vesicles host copper sulphides, such as: bornite with chalcopyrite spindles forming triangular and reticulated patterns (Fig. 15e); digenite, covellite and bornite (Fig. 15f).

Native copper of two types can be distinguished by host mineral and trace-element content. Type 1 is found as fine-grained inclusions in laths of turbid feldspar in amygdaloidal porphyritic basalt (Fig. 16a). Type 2 native copper forms cuprite-rimmed, centimetre-sized aggregates with malachite in altered basaltic rock (Fig. 14b). The feldspar-hosted (Type 1) native copper is rich in sulphur (2000–20263 ppm) and arsenic (146–6017 ppm) compared to Type 2 native copper (149–1288 ppm S, <90–146 As). The silver contents are remarkably higher (<65–2186 ppm Ag in Type 1 and <65–928 ppm Ag in Type 2) than those in native copper from the Keweenaw Peninsula of northern Michigan (Fig. 16b).
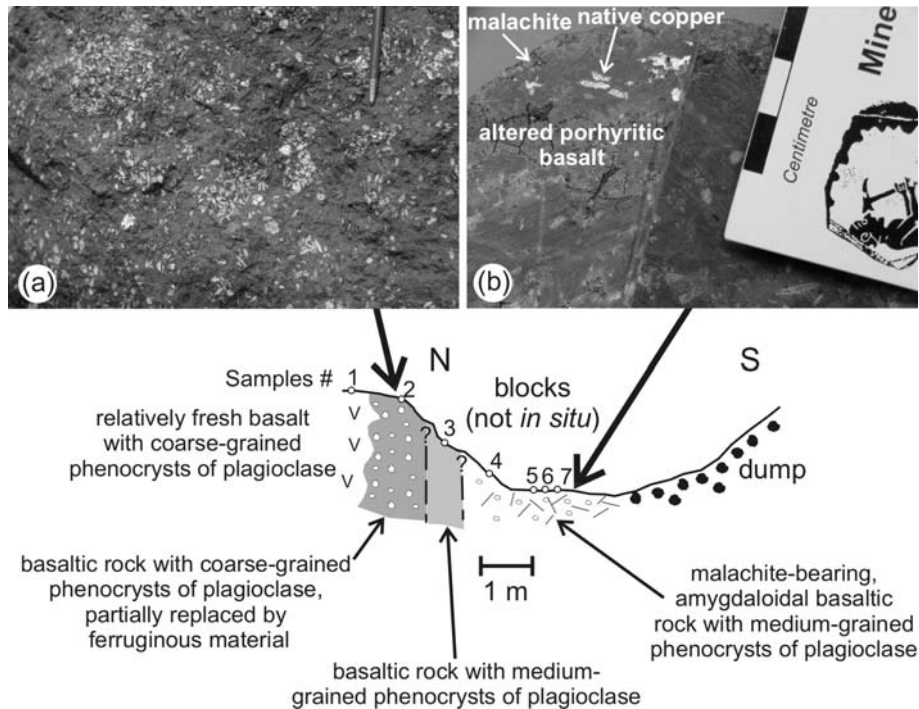
Fig. 14. Schematic section of the quarry working at "Triangle d'Argent". The mineralisation is not *in situ*.

Bulk-rock chemical analyses show compositional variation from marginal to central (mineralised) zones of the quarry (Fig. 17). The $Fe_2O_3/FeO$ ratio is greatest (~10) at the margin and reaches zero in the Type 2 native copper-rich sample in the centre, which has the highest copper content. Sodium is progressively enriched towards the centre, but is notoriously depleted in the Type 2 native copper-rich sample.

### DISCUSSION AND INTERPRETATION

*Transfiguration*

Alpha fabrics indicative of desiccation and expansive growth by evaporation, such as barite- and calcite-filled cracks (Figs. 6a, b), are consistent with groundwater calcretes in arid areas (Wright & Tucker 1991). The nodular calcrete horizon should thus represent palaeogroundwater seepage on the Taconian unconformity, as basement highs are important in ponding drainage (Arakel 1986). The calcrete nodules, which contain minor pyrite and traces of galena and sphalerite, are hosted in greenish sandstone at the base of a greyish sandstone unit within a red-bed succession. Possibly, the calcrete-bearing basal sandstone was never reddened, since

continental red beds are not deposited as originally red sediments (Weibel 1998, Brown 2005 and references therein). By extension, the grey sandstone unit that hosts the Cu–Pb–Zn–Ag mineralisation may have preserved its original colour. This is suggested by relics of greyish areas within reddish sandstone (Fig. 4b), but contradicted by the inverse relationship in which reddish sandstone is bleached (Fig. 4a).

Mineralisation does not occur along the contact between reddish and greyish sandstone units. This would be a suitable reduction–oxidation (redox) boundary for sulphide deposition. Instead, mineralised intervals are located in greyish sandstone without any obvious connection with redox boundaries. On the other hand, the basal contact with Cambro-Ordovician rocks is eventually mineralised where cross-cut by faults (*vide* p. 4). These observations suggest that the cupriferous fluid (assuming that the overlying red-bed sequence is the source of metals, *e.g.*, Brown 2003) was canalised by faults into the subjacent greyish unit where it percolated laterally (*cf.* Lisbon Valley copper deposit, Hitzman *et al.* 2005).

In Llandoverian time (Fig. 18a), the drainage was probably conditioned by the organic carbon-rich Cambro-Ordovician basement (Bertrand & Malo 2001), upon which Na-saturated, reduced groundwater ponded to form nodular calcretes. The
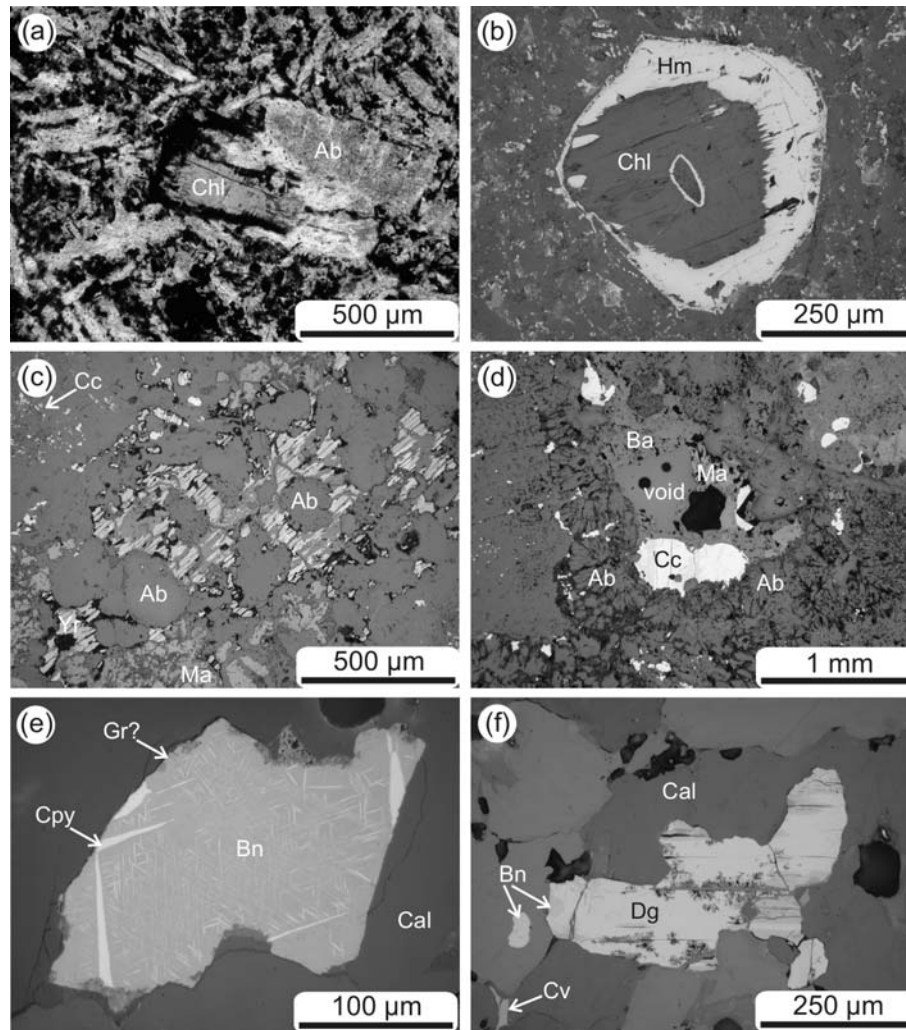
9

Fig. 15. Transmitted- (a) and reflected-light (b–f, air) photomicrographs of altered basaltic rocks. (a) Albitized plagioclase (Ab) partially replaced by chlorite (Chl). (b) Hematite (Hm) substituting chlorite (Chl). (c) Veinlet of radiating albite (Ab), yarrowite (Yr) and malachite (Ma). Chalcocite (Cc) is disseminated in the adjacent groundmass. (d) Void filling by radiating albite (Ab), barite (Ba), chalcocite (Cc) and malachite (Ma). (e) Chalcopyrite lamellae (Cpy) in bornite (Bn), rimmed by a Cu–S phase (geerite?, Gr), in calcite (Cal) vesicle. (f) Digenite (Dg), bornite (Bn) and covellite (Cv) in calcite (Cal) vesicle.

calcrete nodules show pervasive etching and replacement of detrital quartz by calcite (Figs. 6e, f) and, subordinately, by pyrite (Fig. 6d). As quartz is insoluble below a pH of approximately 10, an unlikely high alkalinity for groundwater, organic species could have affected quartz and aluminosilicate stabilities (Surdam *et al*. 1989). The light carbon isotope signature of calcrete calcite could be derived from the degradation of organic matter (Gawthorpe 1987, Mozley & Hoernle 1990, Chan *et al*. 2000).

The negative $\delta^{34}S$ values of sulphides are in the range attributed to bacterial reduction of pore water sulphate (BSR, *e.g.*, Marowsky 1969, Ohmoto & Felder 1987, McGowan *et al.* 2006). Hydrocarbon-bearing fluid inclusions in albite intergrown with low-$\delta^{34}S$ chalcopyrite (-15.2 and -1.2‰) in veinlets and pores could indicate coupled reactions in which pore water sulphate was bacterially reduced and organic carbon was oxidised. Organic carbon may have contributed to vein and cement calcites, which have $\delta^{18}O$ and $\delta^{13}C$ values that overlap with those of calcite precipitated from brines that exchanged with hydrocarbons (Fig. 12). The highest sulphide $\delta^{34}S$ value (25.1‰) is close to that of vein barite (26.2‰), suggesting thermochemical reduction of Silurian sea water sulphate (TSR, *e.g.*, Machel *et al.* 1985, McGowan *et al.* 2006).
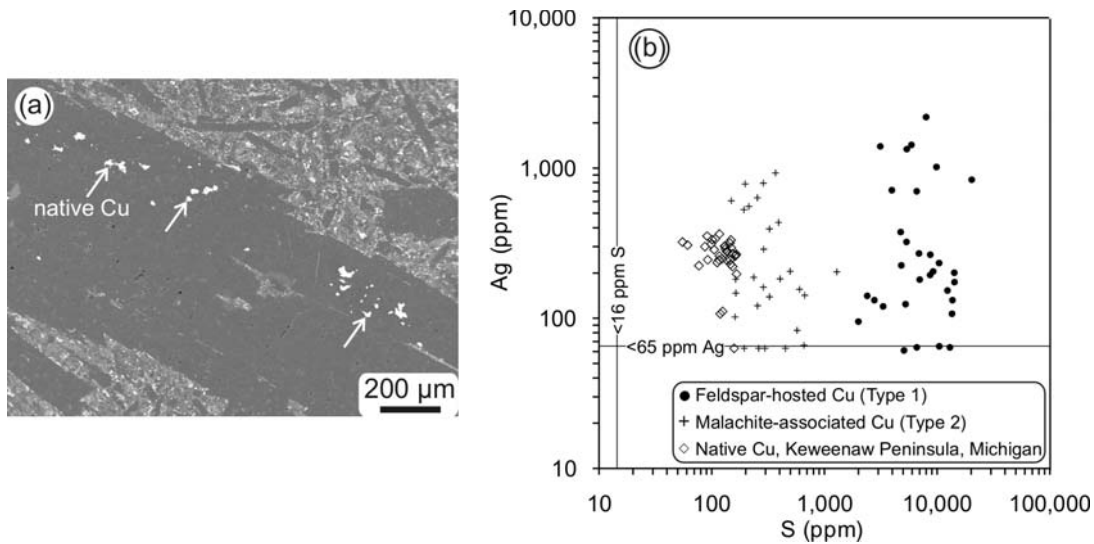
10

Fig. 16. (a) BSE image of native copper (arrows) along the c-axis of a plagioclase phenocryst (dark grey). The groundmass of the basaltic rock is spotted with titanium oxide and hematite (white). (b) S vs. Ag plot of electro-microprobe analyses of native copper.

In the Ludlovian, synsedimentary faulting related to the Salinic disturbance triggered pulses of hydrocarbon-bearing fluids from the Cambro-Ordovician basement into lowermost Silurian rocks (Kirkwood *et al*. 2001, Lavoie & Morin 2004). This scenario is thus tentatively envisaged for the cupriferous mineralisation at Transfiguration (Fig. 18b): pseudomorphic replacement of early pyrite by chalcopyrite (Fig. 7a) and sulphide precipitation in response to interaction between red bed-derived cupriferous fluid and hydrocarbon-bearing basinal brine from underlying Cambro-Ordovician rocks.

*Mont Alexandre*

The presence of argentiferous native copper included in plagioclase (Fig. 16a) is remarkable because its origin is considered to be magmatic (*e.g.*, Nishida *et al.* 1994). Consequently, the basaltic rocks of Mont Alexandre are *per se* the source of metals for the epigenetic Cu–Ag mineralisation.

The cupriferous occurrence investigated here and those described by Duffours (2000) could be classified as 'volcanic red-bed copper' (Kirkham 1996). According to the model advanced by Kirkham, significant part of the volcanic pile must be subaerial to account for oxidation of the volcanic flows. However, as pointed out by Bédard (1986b), the oxidation of the Lac McKay lavas cannot be subaerial for the lavas are interbedded with deep-water sediments (Bourque *et al*. 1995, Bourque 2001). That author suggested that the oxidation could be
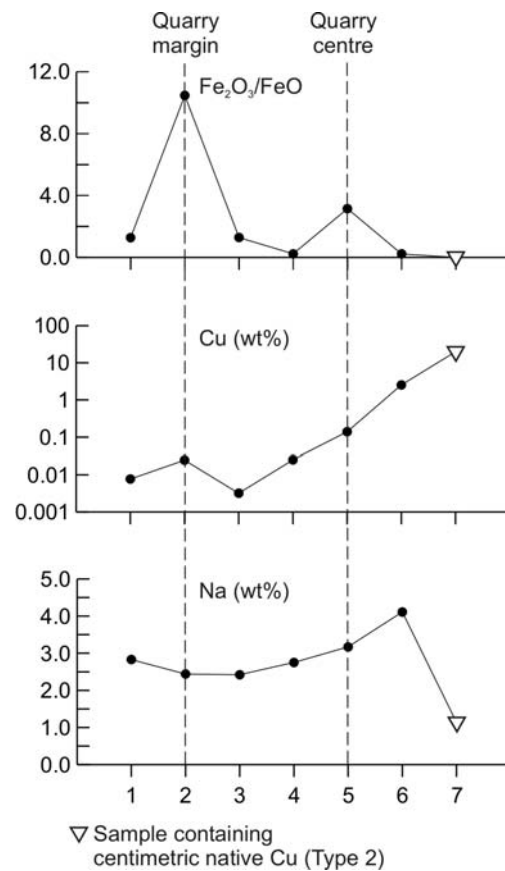


Fig. 17. Variarions of Fe2O3, Cu and Na from the marginal to central zones of the quarry. Numbers refer to samples located in Fig. 14.
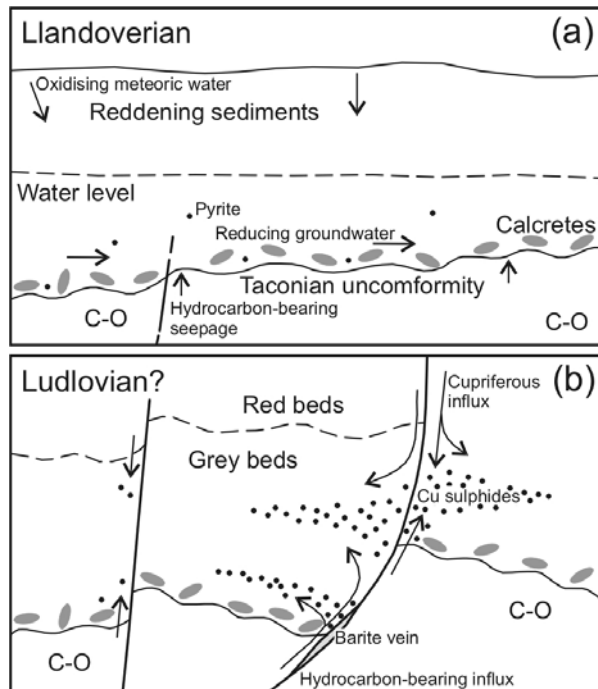
11

Fig. 18. Tentative model for the Transfiguration Cu–Pb–Zn–Ag mineralisation. Arrows indicate fluid migration paths. (a) Ponding of reduced groundwater on the Cambro-Ordovician basement (C-O); calcrete development and formation of BSR pyrite below the water level. (b) Faulting related to Salinic tectonics triggered leakage of hydrocarbon-bearing fluid from the basement, concomitant with cupriferous fluid influx from the overlying red beds. Sulphides were deposited by reaction with early BSR pyrite and by interaction between ascending and descending fluids.

magmatic, but such an origin is unsuitable to explain the sodium metasomatism (albitization) and the chlorite replacement by hematite (Fig. 15b). The latter also conflicts with Duffours' assertion that the spatial association of hematite and chlorite is fortuitous.

The albitization, chloritization and hematitic alteration of the Mont Alexandre basaltic rocks are better understood as a consequence of hydrothermal activity related to sea water infiltration, *i.e.*, spilitisation (Herrmann & Wedepohl 1970, Munhá & Kerrich 1980). Spilitisation provides an explanation for the normative albite (Morin & Simard 1987) and the copper depletion (Dostal *et al.* 1993) in the Late Silurian–Early Devonian basalts of the Gaspé Peninsula. The alteration and cupriferous mineralisation observed at the "Triangle d'Argent" quarry is analogous to the epigenetic native copper hosted by spilitised basaltic flows from La Désirade, Lesser Antilles (Nagle *et al.* 1973). There, the mineralisation is associated with secondary calcite

and hematite in chloritized basalt that was oxidised by heated, oxygenated sea water.

## CONCLUSION

The project has enabled to suggest to:

1. Transfiguration: (i) the greyish sandstone that hosts mineralisation is the result of ponding of reduced groundwater on the Taconian unconformity; (ii) early pyrite formed by bacterial sulphate reduction (BSR) and commonly contains lead in solid solution; (iii) BSR pyrite and mobile hydrocarbon served as reductants for metal deposition as copper, lead and zinc sulphides; (iv) underlying Cambro-Ordovician rocks leaked hydrocarbon-bearing fluid into the Robitaille Formation; (v) fluid leakage from both the basement and superjacent red bed unit probably took place during the Salinic disturbance.

2. Mont Alexandre: (i) basaltic lava contains magmatic native copper included in plagioclase; oxidation of basaltic flows is not related to subaerial environment, but to spilitisation; (ii) spilitisation can account for the anomalous sodium content and copper depletion reported in previous studies; (iii) copper and silver were leached from basalts during spilitisation and ultimately deposited as argentiferous native copper.

## REFERENCES

ARAKEL, A.V. (1986): Evolution of calcrete in palaeodrainages of the Lake Napperby area, central Australia. *Palaeogeography, Palaeoclimatology, Palaeoecology* **54**, 283-303.

BÉDARD, J.H. (1986a): Les suites magmatiques du Paléozoïque supérieur en Gaspésie. Ministère de l'Énergie et des Ressources du Québec, ET 84-09, 111 pp.

BÉDARD, J.H. (1986b): Pre-Acadian magmatic suites of the southeastern Gaspé Peninsula. *Geological Society of America Bulletin* **97**, 1177-1191.

BELLEHUMEUR, C. & VALIQUETTE, G. (1993): Synthèse métallogénique du centre nord de la Gaspésie. Ministère de l'Énergie et des Ressources du Québec, ET 92-03, 65 pp.

BERTRAND, R. & MALO, M. (2001): Source rock analysis, thermal maturation and hydrocarbon generation in Siluro-Devonian rocks of the Gaspé Belt basin, Canada. *Bulletin of Canadian Petroleum Geology* **49**, 238-261.

BOURQUE, P.A. (1975): Lithostratigraphic framework and unified nomenclature for Silurian and basal Devonian rocks in eastern Gaspé Peninsula, Québec. *Canadian Journal of Earth Sciences* **12**, 858-872.

BOURQUE, P.A. (2001): Sea level, synsedimentary tectonics, and reefs: implications for hydrocarbon exploration in the Silurian–lowermost Devonian Gaspé Belt, Québec Appalachians. *Bulletin of Canadian Petroleum Geology* **49**, 217-237.

BOURQUE, P.A. & LACHAMBRE. G. (1980): Stratigraphie du Silurien et du Dévonien basal du sud de la Gaspésie. Ministère de l'Energie et des Ressources du Québec, ES-30, 123 pp.

BOURQUE, P.A., BRISEBOIS, D. & MALO, M. (1995): Gaspé Belt. *In* Geology of the Appalachian-Caledonian orogen in Canada and Greenland (H. Williams, ed.). Geological Survey of Canada, Geology of Canada **6** (316-351).

BOURQUE, P.A., MALO, M. & KIRKWOOD, D. (2001): Stratigraphy, tectono-sedimentary evolution and paleogeography of the post-Taconian–pre-Carboniferous Gaspé Belt: an overview. *Bulletin of Canadian Petroleum Geology* **49**, 186-201.

BROWN, A.C. (1992): Sediment-hosted stratiform copper deposits. *Geoscience Canada* **19**, 125-141.

BROWN, A.C. (2003): Redbeds: source of metals for sediment-hosted stratiform copper, sandstone copper, sandstone lead, and sandstone uranium–vanadium deposits. *In* Geochemistry of sediments and sedimentary rocks: evolutionary considerations to mineral deposit-forming environments (D.R. Lentz, ed.). Geological Association of Canada, GeoText **4** (121-133).

BROWN, A.C. (2005): Refinements for footwall red-bed diagenesis in the sediment-hosted stratiform copper deposits model. *Economic Geology* **100**, 765-771.

CATHELINEAU, M. & NIEVA, D. (1985): A chlorite solid solution geothermometer: the Los Azufres (Mexico) geothermal system. *Contributions to Mineralogy and Petrology* **91**, 235-244.

CHAN, M.A., PARRY, W.T. & BOWMAN, J.R. (2000): Diagenetic hematite and manganese oxides and fault-related fluid flow in Jurassic sandstones, southeastern Utah. *American Association of Petroleum Geologists Bulletin* **84**, 1281-1310.

DOSTAL, J., LAURENT, R. & KEPPIE, J.D. (1993): Late Silurian–Early Devonian rifting during dextral transpression in the southern Gaspé Peninsula (Quebec): petrogenesis of volcanic rocks. *Canadian Journal of Earth Sciences* **30**, 2283-2294.

DUFFOURS, C. (2000): *Minéralisations Cuprifères du Mont Alexandre, Gaspésie*. Unpublished M.Sc. thesis, Université du Québec à Montréal, 125 pp.

GAWTHORPE, R.L. (1987): Burial dolomitization and porosity development in a mixed carbonate–clastic sequence: an example from the Bowland Basin, northern England. *Sedimentology* **34**, 533-558.

HITZMAN, M., KIRKHAM, R.V., BROUGHTON, D., THORSON, J. & SELLEY, D. (2005): The sediment-hosted stratiform copper ore system. *In* Economic Geology 100th anniversary volume (J.W. Hedenquist, J.F.H. Thompson, R.J. Goldfarb, J.P. Richards, eds.). Society of Economic Geologists (609-642).

HERRMANN, A.G. & WEDEPOHL, K.H. (1970): Untersuchungen an spilitischen Gesteinen der variskischen Geosynkline in Nordwestdeutschland. *Contributions to Mineralogy and Petrology* **29**, 255-274

HUPÉ, A. (2001): *Campagne de Forages 2000, Propriété Transfiguration, Secteur Bédard*. Unpublished report, Ressources Appalaches, Rimouski.

JONES, I.W. (1938): Région du Mont Alexandre, Péninsule de Gaspé. Ministère de Mines et de Pêcheries, Québec, Rapport Annuel du Services des Mines de Québec pour l'Année 1936, Partie D (5-28).

KIRKHAM, R.V. (1989): Distribution, settings and genesis of sediment-hosted stratiform copper deposits. *In* Sediment-hosted stratiform copper deposits (R.W. Boyle, A.C. Brown, C.W. Jefferson, E.C. Jowett, & R.V. Kirkham,eds.). Geological Association of Canada, Special Paper **36** (3-38).

KIRKHAM, R.V. (1996): Volcanic redbed copper. *In* Geology of Canadian mineral deposit types (O.R. Eckstrand, W.D. Sinclair & R.I. Thorpe, eds.). Geological Survey of Canada, Geology of Canada **8** (241-252).

KIRKWOOD, D., SAVARD, M.M. & CHI, G. (2001): Microstructural analysis and geochemical vein characterization of the Salinic event and Acadian Orogeny: evaluation of the hydrocarbon reservoir potential in eastern Gaspé. *Bulletin of Canadian Petroleum Geology* **49**, 262-281.

LAURENT, R. & BÉLANGER, J. (1984): Geochemistry of Silurian-Devonian alkaline basalt suites from the Gaspé Peninsula, Quebec Appalachians. *Maritime Sediments and Atlantic Geology* **20**, 67-78.

LAVOIE, D. & MORIN, C. (2004): Hydrothermal dolomitization in the Lower Silurian Sayabec Formation in northern Gaspé–Matapédia (Québec): constraint on timing of porosity and regional significance for hydrocarbon reservoirs. *Bulletin of Canadian Petroleum Geology* **52**, 256-269.

LAVOIE, D., BOURQUE, P.A. & HÉROUX, Y. (1992): Early Silurian carbonate platforms in the Appalachian orogenic belt: the Sayabec–La Vieille formations of the Gaspé–Matapédia basin, Quebec. *Canadian Journal of Earth Sciences* **29**, 704-719.

MACHEL, H.G., KROUSE, H.R. & SASSEN, R. (1995): Products and distinguishing criteria of bacterial and thermochemical sulfate reduction. *Applied Geochemistry* **10**, 373-389.

MALO, M. (2001): Late Silurian–Early Devonian tectono-sedimentary history of the Gaspé Belt in the Gaspé Peninsula: from a transtensional Salinic basin to an Acadian foreland basin. *Bulletin of Canadian Petroleum Geology* **49**, 202-216.

MALO, M. (2004): Paleogeography of the Matapédia basin in the Gaspé Appalachians: initiation of the Gaspé Belt successor basin. *Canadian Journal of Earth Sciences* **41**, 553-570.

MAROWSKY, G. (1969): Schwefel-, Kohlenstoff- und Sauerstoff-Isotopenuntersuchungen am Kupferschiefer als Beitrag zur genetischen Deutung. *Contributions to Mineralogy and Petrology* **22**, 290-334.

McGOWAN, R.R., ROBERTS, S. & BOYCE, A.J. (2006): Origin of the Nchanga copper–cobalt deposits of the Zambian Copperbelt. *Mineralium Deposita* **40**, 617-638.

MORIN, R. & SIMARD, M. (1987): Géologie des régions de Sirois et de Raudin, Gaspésie. Ministère de l'Énergie et des Ressources du Québec, ET 86-06, 69 pp.

MOZLEY, P.S. & HOERNLE, K.A.J. (1990): Geochemistry of carbonate cements in the Sag River and Shublik Formations (Triassic/Jurassic), North Slope, Alaska: implications for the geochemical evolution of formation waters. *Sedimentology* **37**, 817-836.

MUNHÁ, J. & KERRICH, R. (1980): Sea water basalt interaction in spilites from the Iberian Pyrite Belt. *Contributions to Mineralogy and Petrology* **73**, 191-200.

NAGLE, F., FINK, L.K., BOSTRÖM, K. & STIPP, J.J. (1973): Copper in pillow basalts from La Désirade, Lesser Antilles island arc. *Earth and Planetary Science Letters* **19**, 193-197.

NISHIDA, N., KIMATA, M. & ARAKAWA, Y. (1994): Native zinc, copper, and brass in the red-clouded anorthite megacrysts as probes of arc-magmatic process. *Naturwissenschaften* **81**, 498-502.

OHMOTO, H. & FELDER, R.P. (1987): Bacterial activity in the warmer, sulphate-bearing, Archaean oceans. *Nature* **328**, 244-246.

SCHRIJVER, K. & BEAUDOIN, G. (1987): Diverse occurrences of galena-cemented sandstones in the Paleozoic, northern Appalachians, Quebec. *CIM Bulletin* **80** (908), 54-62.

SURDAM, R.C., CROSSEY, L.J., HAGEN, E.S. & HEASLER, H.P. (1989): Organic–inorganic interactions and sandstone diagenesis. *American Association of Petroleum Geologists Bulletin* **73**, 1-23.

WEIBEL, R. (1998): Diagenesis in oxidising and locally reducing conditions – an example from the Triassic Skagerrak Formation, Denmark. *Sedimentary Geology* **121**, 259-276.

WRIGHT, V.P. (1990): A micromorphological classification of fossil and recent calcic and petrocalcic microstructures. *In* Soil Micromorphology: a Basic and Applied Science (L.A. Douglas, ed.). Developments in Soil Science **19**, Elsevier, Amsterdam (401-407).

WRIGHT, V.P. & TUCKER, M.E. (1991): Calcretes: an introduction. *In* Calcretes (V.P. Wright & M.E. Tucker, eds.). International Association of Sedimentologists, Reprint Series **2**, Blackwell Scientific Publications, Oxford (1-22).